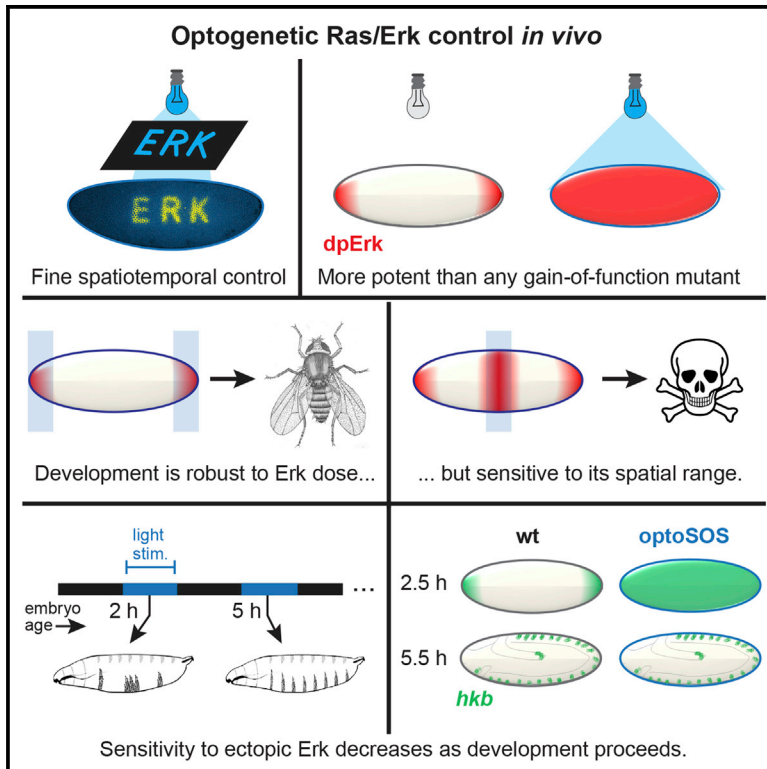


Developmental Cell

The Spatiotemporal Limits of Developmental Erk Signaling

Graphical Abstract



Authors

Heath E. Johnson, Yogesh Goyal,
Nicole L. Pannucci, Trudi Schüpbach,
Stanislav Y. Shvartsman,
Jared E. Toettcher

Correspondence

toettcher@princeton.edu

In Brief

The Ras/Erk pathway plays a conserved and essential role in development. Here, Johnson, Goyal et al. use optogenetics to manipulate Erk signaling in the *Drosophila* embryo, revealing its differential sensitivity to the dose, duration, and spatial range of Erk activity.

Highlights

- Optogenetic inputs can achieve spatiotemporal control of Erk signaling *in vivo*
- Light-induced Erk is more potent than any known gain-of-function mutation
- Development is sensitive to changes in the spatial range but not the dose of Erk
- Late embryogenesis is robust even to global changes in the level of Erk activity



The Spatiotemporal Limits of Developmental Erk Signaling

Heath E. Johnson,^{1,4} Yogesh Goyal,^{2,3,4} Nicole L. Pannucci,¹ Trudi Schüpbach,¹ Stanislav Y. Shvartsman,^{2,3} and Jared E. Toettcher^{1,5,*}

¹Department of Molecular Biology

²Department of Chemical and Biological Engineering

³Lewis-Sigler Institute for Integrative Genomics
Princeton University, Princeton, NJ 08544, USA

⁴Co-first author

⁵Lead Contact

*Correspondence: toettcher@princeton.edu

<http://dx.doi.org/10.1016/j.devcel.2016.12.002>

SUMMARY

Animal development is characterized by signaling events that occur at precise locations and times within the embryo, but determining when and where such precision is needed for proper embryogenesis has been a long-standing challenge. Here we address this question for extracellular signal regulated kinase (Erk) signaling, a key developmental patterning cue. We describe an optogenetic system for activating Erk with high spatiotemporal precision *in vivo*. Implementing this system in *Drosophila*, we find that embryogenesis is remarkably robust to ectopic Erk signaling, except from 1 to 4 hr post-fertilization, when perturbing the spatial extent of Erk pathway activation leads to dramatic disruptions of patterning and morphogenesis. Later in development, the effects of ectopic signaling are buffered, at least in part, by combinatorial mechanisms. Our approach can be used to systematically probe the differential contributions of the Ras/Erk pathway and concurrent signals, leading to a more quantitative understanding of developmental signaling.

INTRODUCTION

The highly conserved extracellular signal regulated kinase (Erk) controls tissue patterning and morphogenesis in developing organisms from flatworms to humans (Umesono et al., 2013; Corson et al., 2003; Gabay et al., 1997a). It is most commonly activated by locally produced growth factors that establish elaborate patterns of signaling, thereby providing spatiotemporal control of cell responses. Studies in model organisms using gain-of-function (GOF) pathway mutations have established that aberrantly increasing Erk activity during development can result in improperly formed and malfunctioning structures (Bruner et al., 1994; Klingler et al., 1988). Consistent with these observations in the laboratory, deregulated Erk activation resulting from activating mutations in the Erk pathway has been associated with a large class of developmental abnormalities in hu-

mans (Jindal et al., 2015; Rauen, 2013). The structural and functional phenotypes observed in affected individuals include congenital heart defects and delayed growth and are believed to result from Erk signaling events that may be too strong, too long, or not sufficiently restricted in space. All of this leads to questions about the sensitivity of the Erk-dependent developmental processes to quantitative changes in Erk activation.

What are the upper limits of signal dose, domain, and duration? Current approaches to addressing these questions rely on genetic perturbations, such as targeted expression systems and conditional mutants, which can augment endogenous signaling patterns. Yet most of these approaches have limited precision and dynamic range, making it difficult or impossible to independently perturb the timing, location, and level of a developmental signal. Here we demonstrate that the power of experimental approaches aimed at addressing this important problem can be significantly increased by optogenetic control. We have developed a versatile approach for perturbing Erk activity in developing organisms and have implemented it in the early *Drosophila* embryo, the model organism that provided the first view of Erk dynamics in developing tissues (Gabay et al., 1997a, 1997b) and continues to provide insights into the quantitative control of the Erk pathway. Our findings reveal that the consequences of increasing Erk signaling are very different depending on whether the intensity, location, or timing of Erk signaling is perturbed. These results help to explain how even the globally activating mutations associated with Erk-related developmental defects lead to highly tissue-specific effects.

RESULTS

Developing Tunable Optogenetic Control of the Ras/Erk Pathway *In Vivo*

Our strategy for spatiotemporal control of developmental Erk signaling is based on inducing the membrane translocation of a Ras activator, SOS, to the plasma membrane with light. Our first efforts to control Erk activity *in vivo* were based on the Phy/PIF approach we previously developed in mammalian cells (Toettcher et al., 2013). Although both the Phy and PIF components were expressed *in vivo* (see Figure S1A), recruitment was poor, and our efforts were limited by the challenge of injecting phycocyanobilin into embryos, which presented a significant

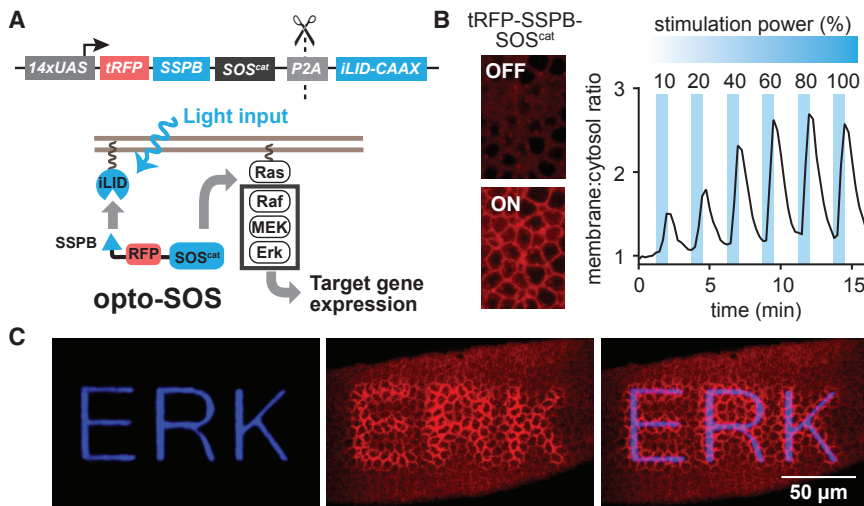


Figure 1. Light-Mediated Activation of Signaling Pathways In Vivo

(A) Schematic of optogenetic control of Erk signaling. An upstream activation sequence drives tissue-specific expression of both optogenetic components, tRFP-SSPB-SOS^{cat} and iLID-CAAX, which are cleaved by a P2A sequence into separate peptides. Recruiting SOS^{cat} to the membrane with light activates the Ras/Erk cascade.

(B) Quantification of membrane SOS^{cat} recruitment over time for varying light intensities.

(C) Local illumination (left panel) can be used to generate spatially precise patterns of membrane SOS^{cat} recruitment (middle and right panels).

See also Figure S1.

experimental burden (Figure S1B). We therefore pursued an alternative strategy based on a blue-light-responsive heterodimerization pair, the iLID/SSPB system, forming the basis of the rest of the current study (Guntas et al., 2015).

This OptoSOS system consists of two components: a light-switchable membrane anchor (iLID-CAAX) and a fluorescent Ras activator (tRFP-SSPB-SOS^{cat}) that is relocalized to the membrane after light stimulation. Both components are expressed from a single construct using a P2A cleavable peptide to generate two protein products from a single transcript (Figure 1A) (Daniels et al., 2014). Because the cleavage of P2A sequences operates with high efficiency in many cellular contexts (Kim et al., 2011), this single-vector strategy is likely to be highly generalizable to other organisms. After verifying that light-induced Erk phosphorylation reached levels comparable to those observed with constitutively active Erk pathway mutations in *Drosophila* S2 cells (see Figure S1C), we used the Gal4-UAS system to uniformly express both OptoSOS components in the early embryo (Duffy, 2002; Hunter and Wieschaus, 2000).

An ideal optogenetic tool for probing developmental signaling should be fast, spatially precise, and usable with a minimum of specialized reagents and equipment. We found that iLID-based control in *Drosophila* meets all these criteria. Upon light stimulation SOS^{cat} relocalized from the cytoplasm to membrane in less than 1 min, an effect that was completely reversed in the dark within 2 min and could be quantitatively varied by tuning the light intensity (Figure 1B; see also Movie S1). By applying spatially restricted patterns of light, we were also able to control SOS^{cat} recruitment with subcellular resolution (Figure 1C; see also Movie S2). In contrast to other recent approaches (Buckley et al., 2016; Guglielmi et al., 2015), precise spatiotemporal control could be achieved without externally supplied chemical cofactors and required relatively conventional imaging equipment (i.e., single-photon excitation using either a 488-nm laser or blue-light-emitting diodes [LEDs]).

Light-Activated Ras Triggers High Erk Activity and Hallmark Transcriptional Responses

In early embryos, the endogenous pattern of Erk activity is established by the localized activation of Torso, a uniformly expressed

receptor tyrosine kinase. This pattern is essential for the localized expression of several zygotic genes, including *tailless* (*tll*), which plays a key role in specifying the structures at the embryonic termini (Pignoni et al., 1990). Prior genetic studies demonstrated that this expansion of Erk signaling has severe consequences for the embryo; GOF mutations in the Torso pathway lead to complete lethality and loss of body segmentation, effects that can be rescued by hypomorphic alleles of Erk or *tll* (Brunner et al., 1994; Klingler et al., 1988). Importantly, even in these GOF mutants, Erk is not activated to a uniform extent across the embryo. In the middle of the embryo, Erk activity reaches only 40% of the maximum level seen in wild-type embryos and signaling at the termini is not increased compared with wild-type (Grimm et al., 2012). Accordingly, *tll* expression in these mutants is partially extended from the poles but does not reach the middle of the embryo (Figure S2A). These limitations have made it impossible to assess how different regions of the embryo interpret the same increased dose of Erk activation.

In contrast to prior GOF mutations, acute light stimulation induces high, spatially uniform Erk activation and downstream gene induction (Figure 2A; see also Figure S2). Quantification across multiple similarly staged embryos revealed that the level of active, doubly phosphorylated Erk (dpErk) is at least 2-fold higher than the maximum level seen in wild-type embryos, whereas dpErk levels in dark conditions were similar to wild-type (Figure 2B). Light-induced Erk was also fully competent to induce transcriptional responses, and expanded the domain of *tll* expression across more than 80% the embryo, connecting the *tll* bands that are normally present at the anterior and posterior ends (Figure 2C).

Even when maternally driven, the OptoSOS system can be used to induce Erk activity in both surface and internal tissues for at least 12 hr after fertilization, enabling us to perturb signaling through much of embryogenesis (Figures 2D and S2D–S2F). However, in older embryos (5–12 hr after fertilization) we observed that a uniformly increased dpErk field was superimposed upon the normal segmental pattern of Erk activity (Figures 2E and S2D), suggesting that tissues either retain the ability to sense further increases in Ras signaling or become differentially responsive as they adopt specific cell fates. Nevertheless, even in 12-hr-old OptoSOS embryos, the lowest level of dpErk

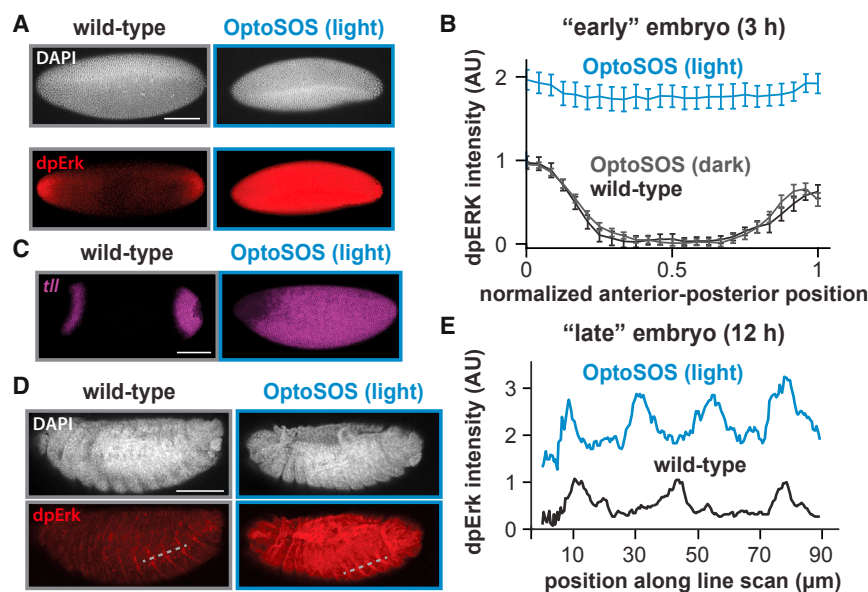


Figure 2. Light Stimulation Induces Global Erk Activity and Downstream Gene Expression

(A) Comparison of Erk activity in wild-type, unstimulated, and light-stimulated OptoSOS embryos at nuclear cycle 14. Embryos were stained for dpErk (red) and DAPI (white). (B) Quantification of dpErk levels from embryos stimulated as in (A) (mean \pm SEM). (C) Fluorescence in situ hybridization for *tailless* (*tll*) in wild-type or light-stimulated OptoSOS embryos at nuclear cycle 14. (D) dpErk activation in 12-hr-old OptoSOS embryos stimulated for 1 hr with light, compared with wild-type embryos of similar age. (E) Quantified dpErk intensity along line scans indicated by the dashed lines in (D). Scale bars, 100 μ m. See Table S1 for numbers of embryos/replicates; see also Figure S2.

between segments was 2- to 3-fold higher than the maximum level observed in wild-type embryos (Figure 2E). Taken together, our results show that the OptoSOS system is highly active in vivo, generating more potent and controllable Erk activity than any known GOF pathway mutation.

Early Embryogenesis Is Sensitive to the Spatial Distribution of Erk Activity but Not Its Dose

Developmental Erk signaling is tightly controlled from embryo to embryo, exhibiting highly reproducible profiles in intensity, spatial range, and duration (Lim et al., 2015). Which of these three features are essential for development? We first focused on intensity, reasoning that if the precise level of Erk activity at the poles was readout by downstream processes, then perturbing that level should be deleterious to development. Such experiments were previously impossible, as no known pathway mutation is capable of generating increased dpErk at the poles.

We applied light to the anterior pole, posterior pole, or center of each embryo during the time at which Erk is normally activated at the termini (Figures 3A and 3B). Embryos stimulated with light only at the termini were viable, producing larvae, pupae, and adult flies that were indistinguishable from wild-type or dark-incubated OptoSOS embryos (Figures S3A and S3B). Furthermore, despite strong light-induced Erk activity in pole cells (Figure S2), which are normally devoid of Erk activity at this point of embryogenesis, termini-illuminated flies were still fertile and had normal gonads (Figure S3B). In contrast, activating Erk in the middle of the embryo disrupted both the early steps of embryonic patterning and subsequent stages of embryogenesis, resulting in complete embryonic lethality similar to that obtained by GOF Torso signaling mutants (Klingler et al., 1988). Strikingly, we found that reducing ectopic activation even to a narrow 40- μ m strip delivered to the middle of the embryo, a region comprising about three to five cell diameters, induced high levels of embryonic lethality (Figure 3C).

To investigate this differential sensitivity in more detail, we examined how different Erk patterns affected the formation of

cuticle structures. Inappropriate Erk activity is known to interfere with cuticle formation and patterning, and strong GOF mutations in Torso signaling induce fusion of embryonic segments or lead to their loss in an Erk-dependent fashion (Figure 3D; see also Figure S3) (Urban et al., 2004; Nussleinvolhard et al., 1984). Consistent with this classic phenotype, the overwhelming majority of embryos illuminated in the center lacked segments, while the remainder exhibited pronounced fusions (Figure 3E). Spatially restricted optogenetic stimulation thus revealed that two regions of the early embryo respond very differently to the same dose of additional Erk activity: the terminal regions (where Erk is normally active) are unaffected, but the middle of the embryo (where the Erk pathway is normally silent) is extremely sensitive.

Our findings can be interpreted in terms of the current model of Torso signaling, according to which Torso-dependent Erk activation controls gene expression by relieving transcriptional repression by Capicua (Cic), a DNA-binding factor that is uniformly expressed in the embryo in the absence of Torso signaling (Jimenez et al., 2000). Downregulation of Cic at the poles is essential for the expression of genes such as *tll* and differentiation into terminal structures such as the posterior midgut, which undergoes contraction and invagination at the onset of gastrulation. At the same time, Cic is needed in the middle of the embryo to play a role in the regulation of the segmentation cascade (Jimenez et al., 2000). Accordingly, adding Erk signaling at the poles does not add much to the anti-repressive effect that is already provided by the endogenous localized activation of Torso, whereas increased Erk signaling (and thus removal of the Cic repressor) in the middle of the embryo has a major effect on the segmentation cascade and results in lethality. Indeed, measuring Cic levels in light-stimulated OptoSOS embryos revealed that nuclear Cic is reduced at all positions along the anterior-posterior axis when compared with wild-type embryos (Figures 3F and 3G), consistent with Cic's role as a target for Erk-mediated degradation.

To gain insight into the underlying developmental processes that are affected by ectopic Ras/Erk signaling, we performed

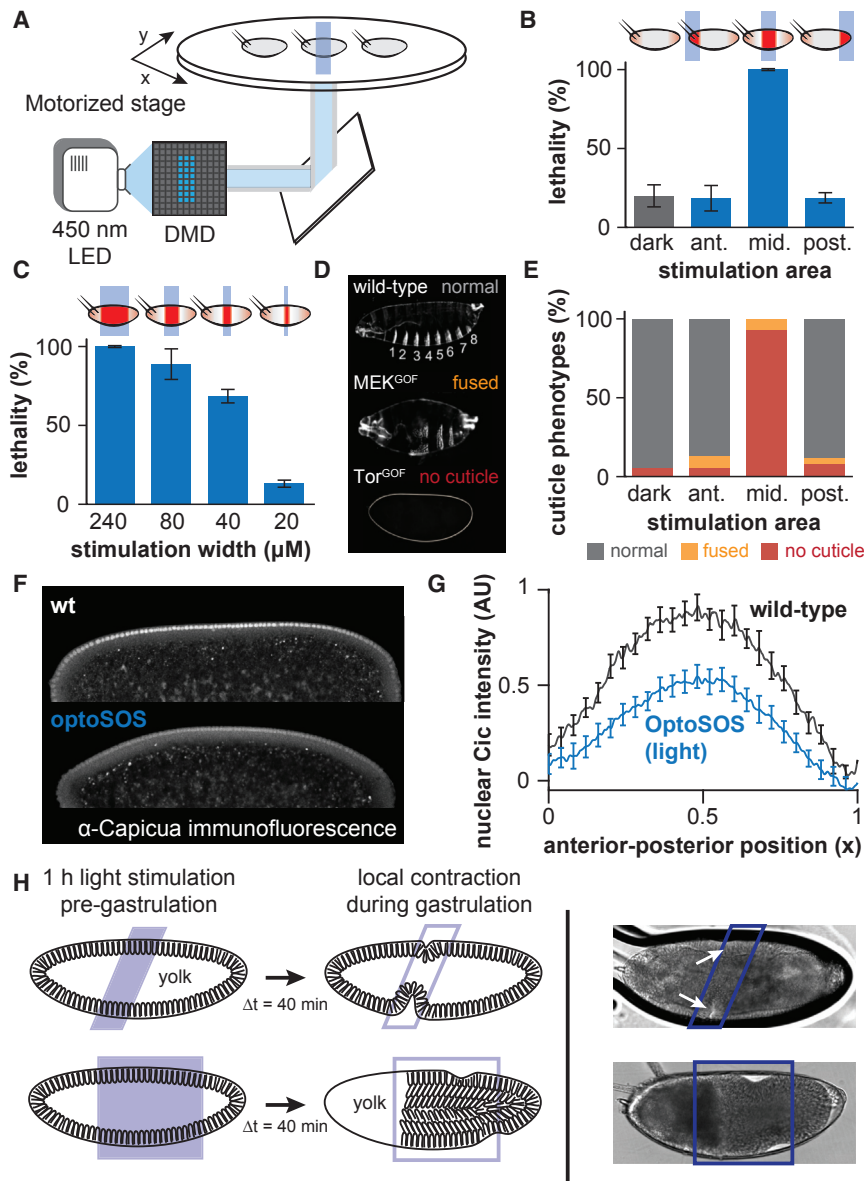


Figure 3. Consequences of Perturbing the Level and Location of Erk Activity

(A) Schematic of the experiment whereby a digital micromirror device was used to apply spatially patterned light to each embryo.

(B) Lethality of local Erk activation from 1 to 3 hr post fertilization (mean ± SD). Light was applied to ~15% of the embryo at a pole, or the middle ~45% of the embryo. The number of hatched larvae was counted.

(C) Lethality after illuminating progressively decreasing stimulation areas in the middle of the embryo (mean ± SD).

(D) Cuticle phenotypes from GOF mutations in the Erk pathway (Tor^{GOF} and Mek^{GOF}).

(E) Quantification of cuticle phenotypes from the experiment shown in (A).

(F) Capicua staining in WT and OptoSOS embryos after 1 hr of illumination.

(G) Quantification of Capicua staining as shown in (F) (mean ± SEM).

(H) Left panels: schematic of experiment. OptoSOS embryos were spatially illuminated during nuclear cycles 13–14, and observed through gastrulation. Right panel: still images of OptoSOS embryos exhibiting tissue contraction during gastrulation. White arrows indicate sites of tissue contraction.

See Table S1 for numbers of embryos/replicates; see also Figure S3.

Embryonic Sensitivity to Ectopic Erk Is Limited to a Narrow Time Window

We have shown that early embryogenesis is insensitive to increased Erk activity at the poles and yet highly sensitive to Erk signaling in the middle of the embryo. Do other developmental stages have a similar Achilles’ heel? To address this question we applied uniform illumination to embryos at different times during development. After collecting freshly laid embryos over a 45-min window, we incubated the embryos in the dark for a specified amount of time (“X hr”), illuminated them for a fixed duration (“Y hr”), and returned them to the dark to complete embryogenesis (Figure 4A). As expected, global illumination of early embryos was lethal and led to segment fusion or loss (Figures 4B and 4C; see also Figure S4). Surprisingly, however, these phenotypes were limited to a brief time window. By 3–4 hr post fertilization, a global increase in Erk activation had no effect on segmentation and cuticle development (Figure 4D). We observed a similar decrease in overall lethality in late-illuminated embryos. Whereas only ~40% of embryos survived global Erk activation induced by low-intensity blue-light exposure during the first 4 hr of embryogenesis, ~75% survived the same light stimulus applied during the rest of embryogenesis, from 4 hr post fertilization until hatching (Figure 4E; see also Figure S4C). We previously found that Erk phosphorylation was induced by light to similar levels above wild-type for at least 12 hr (Figures 2D, 2E,

time-lapse microscopy after local illumination in different regions of the embryo. In center-illuminated OptoSOS embryos but not wild-type embryos, we found that local illumination triggered pronounced tissue invagination at the locations where the light stimulus had previously been applied (Figure 3H; see also Movies S3 and S4). We found that the domain of contraction scaled with the size of the light stimulus: a larger region of light stimulation led to large-scale contraction of the majority of the embryo, ejecting the yolk to the anterior side of the embryo (Figure 3H; see also Movies S5 and S6). This contraction occurred during gastrulation at the same time as invagination of the posterior midgut, and could occur 30 min or more after light stimulation ceased. Our results thus demonstrate that light-activated Ras signaling locally drives the improper specification of contractile tissue, leading to defects in gastrulation that disrupt the normal course of morphogenesis.

As expected, global illumination of early embryos was lethal and led to segment fusion or loss (Figures 4B and 4C; see also Figure S4). Surprisingly, however, these phenotypes were limited to a brief time window. By 3–4 hr post fertilization, a global increase in Erk activation had no effect on segmentation and cuticle development (Figure 4D). We observed a similar decrease in overall lethality in late-illuminated embryos. Whereas only ~40% of embryos survived global Erk activation induced by low-intensity blue-light exposure during the first 4 hr of embryogenesis, ~75% survived the same light stimulus applied during the rest of embryogenesis, from 4 hr post fertilization until hatching (Figure 4E; see also Figure S4C). We previously found that Erk phosphorylation was induced by light to similar levels above wild-type for at least 12 hr (Figures 2D, 2E,

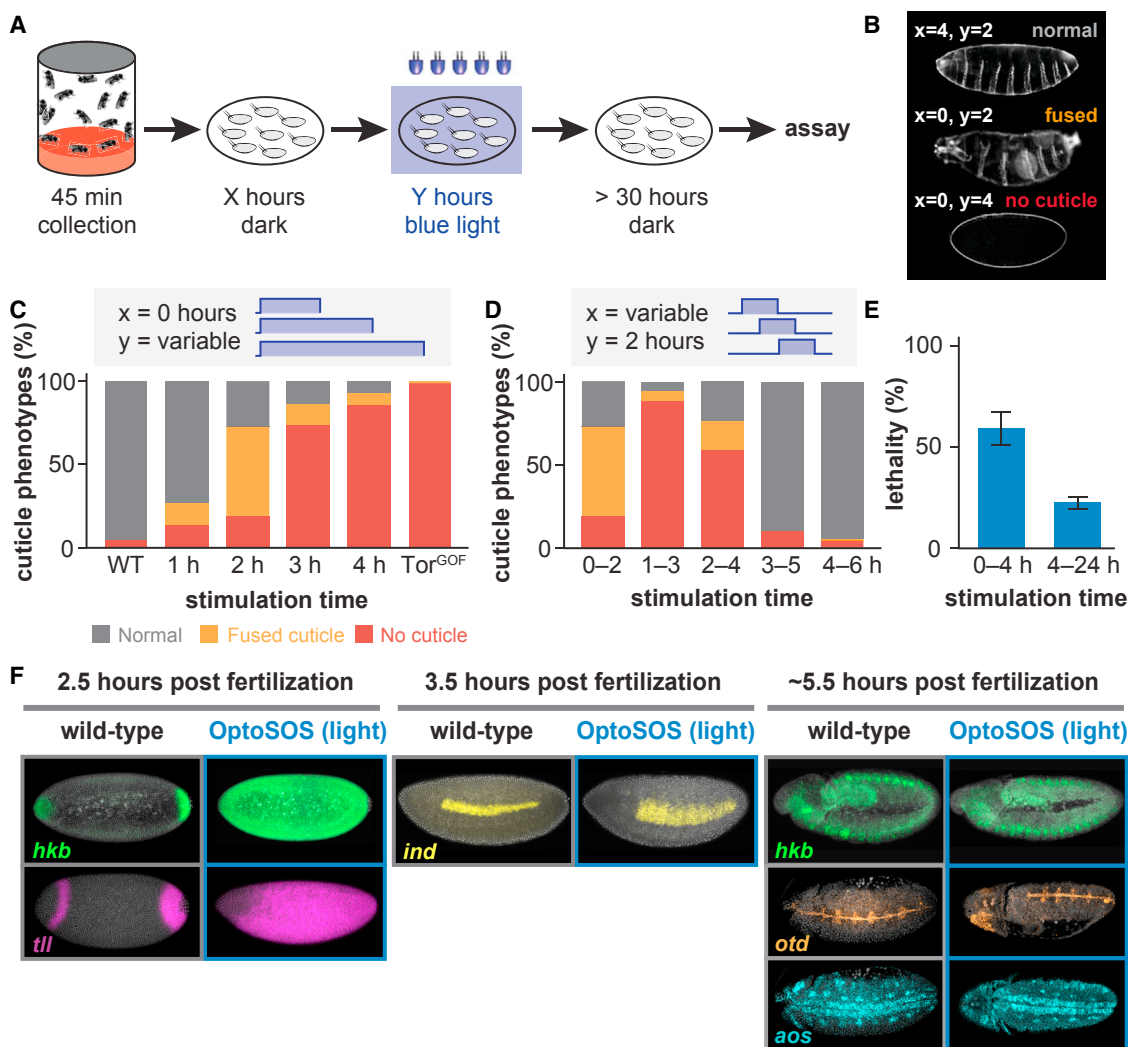


Figure 4. A Temporal Window of Sensitivity to Ectopic Erk Activation

(A) Embryos are collected for 45 min after which they are placed in the dark for X hr before being stimulated globally for Y hr under blue light. After allowing sufficient time to hatch, embryos are then assayed for lethality and segmentation defects.

(B) Examples of cuticle phenotypes obtained by varying light-exposure duration and start time.

(C and D) Quantification of cuticle defects obtained by varying light duration (C) or start time (D), compared with wild-type and a Tor^{GOF} mutant.

(E) Quantification of lethality after stimulation with an intermediate light intensity from 0 to 4 hr after collection versus from 4 hr until hatching (mean ± SEM).

(F) Fluorescence in situ hybridization for *hkb*, *tll*, *ind*, *otd*, and *aos* at the indicated developmental stages for wild-type and light-illuminated OptoSOS embryos. See Table S1 for numbers of embryos/replicates; see also Figure S4.

S2E, and S2F), suggesting that these results are not due to loss of expression of the maternally driven OptoSOS system.

Why might spatial sensitivity be lost at later stages, when we observe that increasing Erk activity no longer has such severe consequences? In contrast to early development, the cells in later embryos have many concurrent sources of positional information: they may already have adopted a specific fate, may alter their sensitivity to signaling inputs by expressing positive or negative regulators, or may have modified chromatin elements on target promoters, or multiple patterning cues may provide additional context (Lim et al., 2015; Lander, 2007; Nguyen et al., 1998). We therefore reasoned that in late embryogenesis, Erk target genes may be subject to combinatorial regulation by

other input pathways, providing additional safeguards that cannot be overridden by ectopic Erk activation.

To test this model, we measured the expression domain of Erk-induced genes at different developmental stages: *huckebein* (*hkb*), *intermediate neuroblasts defective* (*ind*), *orthodenticle* (*otd*), and *argos* (*aos*). In each case, we compared wild-type embryos with blue-light-illuminated OptoSOS embryos, which globally activate Erk signaling. For those genes that are induced in 2.5- to 3-hr-old embryos (*tll* and *hkb*), we observed a dramatic expansion after blue-light stimulation (Figure 4F, left panel). In contrast, light stimulation of 5.5-hr-old OptoSOS embryos induced gene expression that is indistinguishable from similarly aged wild-type embryos (*hkb*; *otd* in 11 of 12 embryos tested),

or that is partially expanded (*aos*; *otd* in 1 of 12 embryos) (Figure 4F, right panel). Finally, for *ind*, an Erk target expressed at an intermediate time (3.5 hr), we observed an intermediate level of expansion (Figure 4F, middle panel). This pattern is consistent with known mechanisms of *ind*'s combinatorial control, including activation by Dorsal and repression by Vnd and Snail (Lim et al., 2013). Our data thus support a model in which Erk activity is initially sufficient to induce downstream gene expression at any embryonic position, but where combinations of positional cues or crosstalk from additional signaling pathways correct quantitative defects in Erk activity at subsequent developmental stages.

DISCUSSION

Twenty years ago, antibody staining revealed a highly dynamic atlas of Erk activation during *Drosophila* embryogenesis (Gabay et al., 1997a, 1997b). Here, we use an optogenetic approach to examine the consequences of perturbing this atlas at different times and spatial locations. We find that throughout embryogenesis, proper development is remarkably robust to perturbations in the level of Erk activity. In contrast, early embryos are extremely sensitive to the location of Erk activity; even a narrow strip of ectopic Erk activity is sufficient to completely halt normal developmental progress. The results we describe are unlike what would be predicted for classical morphogens, in which different genes are thought to be induced at various concentrations of a diffusible factor. Our data are more consistent with Erk activation in the early embryo behaving like a switch, where input levels are unimportant as long as they are above a triggering threshold (Ferrell and Machleder, 1998).

Importantly, our ability to characterize the consequences of increased Erk signaling was only possible because optogenetic stimulation generates such potent, uniform Erk activity in the early embryo (Figures 2A and 2B). This finding was unanticipated and contrasts with results from constitutively active Erk pathway mutations that have been previously studied in the early *Drosophila* embryo (Grimm et al., 2012), which neither increased Erk activity at the embryo termini nor induced Erk activity in the middle of the embryo to high, termini-like levels. This difference may be due to the different time scales of action between light stimulation and genetic perturbation. Long-term activation may desensitize a signaling pathway such as Ras/Erk over time, an effect that may be bypassed by acute stimulation (Hoeller et al., 2016). Optogenetic stimulation may thus serve as a powerful tool even for pathways that have been intensely studied using GOF signaling mutations, potentially revealing new activity states and modes of regulation.

The sensitivity differences we observe between early and late embryos do not arise because Erk signaling is less critical in later development. Indeed, prior loss-of-function studies demonstrated that eliminating Erk patterns at these stages is both lethal and prevents cuticle formation (Klambt et al., 1992; Price et al., 1989; Schejter and Shilo, 1989). Yet our results suggest that the consequences of hyperactive Erk signaling may be more complex than might have been expected from prior genetic studies. For instance, during tracheal development, hyperactivation of the *Drosophila* fibroblast growth factor receptor homolog Btl in tracheal cells stalls migration and tracheal development

(Gabay et al., 1997b; Sutherland et al., 1996). In contrast, we found that OptoSOS larvae that hatch after illumination from 4 to 24 hr of embryogenesis showed no gross defects in tracheal development (Figure S4E). Similarly, the expression patterns of *aos* and *otd* are strongly expanded in the presence of the constitutively active epidermal growth factor ligand *s-spitz* (Schweitzer et al., 1995) but are less perturbed by illumination in OptoSOS embryos (Figure 4F). These differences may point to a hitherto unappreciated role for other pathways that are activated at the receptor level but not by Ras (Toettcher et al., 2013), such as phosphoinositide-dependent signaling, which has recently been implicated in tracheal development (Ghabrial et al., 2011). Alternatively, target gene expression may respond to a feature of Erk activity other than its absolute level. We observed that globally illuminated OptoSOS embryos still exhibited spatial patterns of Erk activity on top of an elevated background (Figure 2E); these patterns may thus still preserve information about the appropriate range for downstream gene expression. Dissecting the mechanisms with which Erk activity is decoded by downstream genes in the developing embryo will be an important challenge for future studies.

Our data suggest that the consequences of Erk hyperactivation are tissue and stage specific, an observation that closely resembles what is observed in human developmental disorders caused by GOF mutations in the Erk pathway. Even uniformly expressed mutant alleles only lead to certain defects in highly specialized tissues (Gelb and Tartaglia, 2011; Pagani et al., 2009), suggesting that many Erk-dependent signaling events may be similarly buffered in vertebrate development. In future work, cellular optogenetics could be useful for revealing the details of this buffering logic by directly setting the activity state of specific input pathways and monitoring the resulting transcriptional responses. Such approaches highlight the potential for optogenetics to reveal how inductive signals are interpreted in space and time.

EXPERIMENTAL PROCEDURES

Plasmids

The tRFP-SSPB-SOScat-P2A-iLID-CAAX expression cassette was first assembled using a PUWR backbone (Drosophila Genome Resource Center, #1281) as transfer vector. The tRFP-SSPB fragment was derived from pLL7.0: tgRFPt-SSPB WT (a gift from Brian Kuhlman, Addgene plasmid #60415). The SOScat fragment was derived from pHR-YFP-PIF-SOScat (Addgene plasmid #50851). The iLID-CAAX sequence was derived from pLL7.0: Venus-iLID-CAAX (a gift from Brian Kuhlman, Addgene plasmid #60411). All fragments were ligated and transferred to the pTIGER vector (Ferguson et al., 2012) using In-Fusion assembly (Clontech).

Fly Procedures

For generation of transgenic flies and stocks, the constructs described above were integrated into the third chromosome using the ϕ C31-based integration system (Bischof et al., 2007), at the Attp site estimated to be at 68A4. OregonR, Histone-GFP, *Tor*^{D4021/+} alleles were also used in the experiments. P(mat α -GAL-VP16)mat67; P(mat α -GAL-VP16)mat15 was used to drive iLIDnano expression in the early embryo (Hunter and Wieschaus, 2000). Flies were raised under standard conditions and crosses were performed at 25°C unless otherwise specified.

Immunostaining and Fluorescence In Situ Hybridization

Rabbit anti-dpErk (1:100; Cell Signaling), rabbit anti-Capicua (1:100; gift from Celeste Berg), sheep anti-GFP (1:1,000, Bio-Rad), sheep anti-digoxigenin

(DIG) (1:125; Roche), mouse anti-biotin (1:125; Jackson ImmunoResearch), rat anti-mCherry (1:1,000; Life Technologies) and rat anti-HA (1:100, Roche #11-867-423-001) were used as primary antibodies. DAPI (1:10,000; Vector Laboratories) was used to stain for nuclei, and Alexa Fluor conjugates (1:500; Invitrogen) were used as secondary antibodies. Fluorescent imaging was done with a Nikon A1-RS scanning confocal microscope with a 20× objective. For pairwise comparisons of wild-type and mutant backgrounds, embryos were collected, stained, and imaged together under the same experimental conditions. Error bars in the figures represent the SEM of embryo ages (x axis) and normalized dpErk intensities (y axis).

Cuticle Preparation

Embryos were dechorionated after being aged for more than 30 hr. Dechorionated embryos were incubated overnight in a medium containing lactic acid and Hoyer's medium (1:1) at 65°C. Cuticle imaging was performed with Nikon Eclipse Ni at 10× objective.

Microscopy

For Figures 1 and S2C, bright-field and confocal microscopy was performed on a Nikon Eclipse Ti spinning-disk confocal microscope (see Supplemental Experimental Procedures for details). For translocation experiments, embryos were dechorionated in 50% bleach for 2 min and rinsed in water before mounting and imaging at 40×. Microscopy of fixed samples in Figures 2 and 3 was performed using a Nikon A1 RS point-scanning confocal microscope (Princeton Microscopy Core). For cuticle staining, dark-field images were collected on a Nikon Eclipse Ni.

For the patterned illumination experiments in Figure 3 and Movie S3, embryos were collected for 45 min, aligned on a coverslip in a 3:1 mix of halo-carbon 700/27 oil. The slide was then sandwiched with a Teflon window chamber using vacuum grease (a technique described in detail in Kiehart et al., 1994). Patterned optogenetic illumination was performed using a Mightex Polygon digital micromirror device using an X-Cite XLED 450-nm blue-light source. Light (450 nm) was applied at 40% power for 100 ms to each embryo at 20×. All embryos were illuminated once every 40 s starting 30 min after collection. At this imaging frequency, up to 30 embryos could be illuminated per experiment. Just before stimulation, differential interference contrast images of each embryo were collected with a 650-nm long-pass filter (Chroma) in the light path to prevent any light-induced SOScat activation. Embryos which were in late nuclear cycle 14 or older were excluded from counts.

Temporal Activation Experiments

Embryos were collected for 45 min at 25°C before being wrapped in foil and aged at room temperature for X hr before stimulation (where X is defined for specific experiments in the corresponding text and figures). They were then placed in blue LED-containing foil-wrapped boxes and stimulated for Y hr before returning to the dark for at least 30 hr (where Y is defined for specific experiments in the corresponding text and figures). The LEDs were toggled on for 1-s pulses at regular intervals using an Arduino microcontroller to achieve lower activation levels. Lethality was calculated by counting unhatched and empty eggshell cases on a random region of each plate.

SUPPLEMENTAL INFORMATION

Supplemental Information includes Supplemental Experimental Procedures, four figures, one table, and six movies and can be found with this article online at <http://dx.doi.org/10.1016/j.devcel.2016.12.002>.

AUTHOR CONTRIBUTIONS

H.E.J., Y.G., T.S., S.Y.S., and J.E.T. conceived and designed the project. H.E.J. and Y.G. performed experiments in flies and cell lines, and H.E.J. and N.L.P. cloned the constructs. J.E.T. wrote the manuscript with input from all authors.

ACKNOWLEDGMENTS

We thank members of the Toettcher and Shvartsman laboratories for comments and suggestions throughout this work, and Kei Yamaya for her help

with fly husbandry. We also thank Celeste Berg (University of Washington) for the Capicua antibody and Amin Ghabrial (University of Pennsylvania) for valuable comments. H.E.J. was supported by NIH Ruth Kirschstein fellowship F32GM119297. This work was also supported by NIH grants R01GM077620 (T.S.), R01GM086537 (S.Y.S. and Y.G.), and DP2EB024247 (J.E.T.). We also thank Dr. Gary Laevsky and the Molecular Biology Microscopy Core, which is a Nikon Center of Excellence, for microscopy support.

Received: August 24, 2016

Revised: October 30, 2016

Accepted: December 1, 2016

Published: January 23, 2017

REFERENCES

- Bischof, J., Maeda, R.K., Hediger, M., Karch, F., and Basler, K. (2007). An optimized transgenesis system for *Drosophila* using germ-line-specific phiC31 integrases. *Proc. Natl. Acad. Sci. USA* *104*, 3312–3317.
- Brunner, D., Oellers, N., Szabad, J., Biggs, W.H., 3rd, Zipursky, S.L., and Hafen, E. (1994). A gain-of-function mutation in *Drosophila* MAP kinase activates multiple receptor tyrosine kinase signaling pathways. *Cell* *76*, 875–888.
- Buckley, C.E., Moore, R.E., Reade, A., Goldberg, A.R., Weiner, O.D., and Clarke, J.D. (2016). Reversible optogenetic control of subcellular protein localization in a live vertebrate embryo. *Dev. Cell* *36*, 117–126.
- Corson, L.B., Yamanaka, Y., Lai, K.M., and Rossant, J. (2003). Spatial and temporal patterns of ERK signaling during mouse embryogenesis. *Development* *130*, 4527–4537.
- Daniels, R.W., Rossano, A.J., Macleod, G.T., and Ganetzky, B. (2014). Expression of multiple transgenes from a single construct using viral 2A peptides in *Drosophila*. *PLoS One* *9*, e100637.
- Duffy, J.B. (2002). GAL4 system in *Drosophila*: a fly geneticist's Swiss army knife. *Genesis* *34*, 1–15.
- Ferguson, S.B., Blundon, M.A., Klovstad, M.S., and Schupbach, T. (2012). Modulation of gurken translation by insulin and TOR signaling in *Drosophila*. *J. Cell Sci.* *125*, 1407–1419.
- Ferrell, J.E., Jr., and Machleder, E.M. (1998). The biochemical basis of an all-or-none cell fate switch in *Xenopus* oocytes. *Science* *280*, 895–898.
- Gabay, L., Seger, R., and Shilo, B.Z. (1997a). In situ activation pattern of *Drosophila* EGF receptor pathway during development. *Science* *277*, 1103–1106.
- Gabay, L., Seger, R., and Shilo, B.Z. (1997b). MAP kinase in situ activation atlas during *Drosophila* embryogenesis. *Development* *124*, 3535–3541.
- Gelb, B.D., and Tartaglia, M. (2011). RAS signaling pathway mutations and hypertrophic cardiomyopathy: getting into and out of the thick of it. *J. Clin. Invest.* *121*, 844–847.
- Ghabrial, A.S., Levi, B.P., and Krasnow, M.A. (2011). A systematic screen for tube morphogenesis and branching genes in the *Drosophila* tracheal system. *PLoS Genet.* *7*, e1002087.
- Grimm, O., Sanchez Zini, V., Kim, Y., Casanova, J., Shvartsman, S.Y., and Wieschaus, E. (2012). Torso RTK controls Capicua degradation by changing its subcellular localization. *Development* *139*, 3962–3968.
- Guglielmi, G., Barry, J.D., Huber, W., and De Renzis, S. (2015). An optogenetic method to modulate cell contractility during tissue morphogenesis. *Dev. Cell* *35*, 646–660.
- Guntas, G., Hallett, R.A., Zimmerman, S.P., Williams, T., Yumerefendi, H., Bear, J.E., and Kuhlman, B. (2015). Engineering an improved light-induced dimer (iLID) for controlling the localization and activity of signaling proteins. *Proc. Natl. Acad. Sci. USA* *112*, 112–117.
- Hoeller, O., Toettcher, J.E., Cai, H., Sun, Y., Huang, C.-H., Freyre, M., Zhao, M., Devreotes, P.N., and Weiner, O.D. (2016). Gβ regulates coupling between actin oscillators for cell polarity and directional migration. *PLoS Biol.* *14*, e1002381.

- Hunter, C., and Wieschaus, E. (2000). Regulated expression of *nullo* is required for the formation of distinct apical and basal adherens junctions in the *Drosophila* blastoderm. *J. Cell Biol.* *150*, 391–401.
- Jimenez, G., Guichet, A., Ephrussi, A., and Casanova, J. (2000). Relief of gene repression by torso RTK signaling: role of *capicua* in *Drosophila* terminal and dorsoventral patterning. *Genes Dev.* *14*, 224–231.
- Jindal, G.A., Goyal, Y., Burdine, R.D., Rauen, K.A., and Shvartsman, S.Y. (2015). RASopathies: unraveling mechanisms with animal models. *Dis. Model. Mech.* *8*, 1167.
- Kiehart, D.P., Montague, R.A., Rickoll, W.L., Foard, D., and Thomas, G.H. (1994). High-resolution microscopic methods for the analysis of cellular movements in *Drosophila* embryos. *Methods Cell Biol.* *44*, 507–532.
- Kim, J.H., Lee, S.R., Li, L.H., Park, H.J., Park, J.H., Lee, K.Y., Kim, M.K., Shin, B.A., and Choi, S.Y. (2011). High cleavage efficiency of a 2A peptide derived from porcine teschovirus-1 in human cell lines, zebrafish and mice. *PLoS One* *6*, e18556.
- Klambt, C., Glazer, L., and Shilo, B.Z. (1992). *breathless*, a *Drosophila* FGF receptor homolog, is essential for migration of tracheal and specific midline glial cells. *Genes Dev.* *6*, 1668–1678.
- Klingler, M., Erdelyi, M., Szabad, J., and Nusslein-Volhard, C. (1988). Function of *torso* in determining the terminal Anlagen of the *Drosophila* embryo. *Nature* *335*, 275–277.
- Lander, A.D. (2007). Morpheus unbound: reimagining the morphogen gradient. *Cell* *128*, 245–256.
- Lim, B., Samper, N., Lu, H., Rushlow, C., Jimenez, G., and Shvartsman, S.Y. (2013). Kinetics of gene derepression by ERK signaling. *Proc. Natl. Acad. Sci. USA* *110*, 10330–10335.
- Lim, B., Dsilva, C.J., Levario, T.J., Lu, H., Schupbach, T., Kevrekidis, I.G., and Shvartsman, S.Y. (2015). Dynamics of inductive ERK signaling in the *Drosophila* embryo. *Curr. Biol.* *25*, 1784–1790.
- Nguyen, M., Park, S., Marques, G., and Arora, K. (1998). Interpretation of a BMP activity gradient in *Drosophila* embryos depends on synergistic signaling by two type I receptors, SAX and TKV. *Cell* *95*, 495–506.
- Nussleinvolhard, C., Wieschaus, E., and Kluding, H. (1984). Mutations affecting the pattern of the larval cuticle in *Drosophila melanogaster*. 1. Zygotic loci on the 2nd chromosome. *Roux Arch. Dev. Biol.* *193*, 267–282.
- Pagani, M.R., Oishi, K., Gelb, B.D., and Zhong, Y. (2009). The phosphatase SHP2 regulates the spacing effect for long-term memory induction. *Cell* *139*, 186–198.
- Pignoni, F., Baldarelli, R.M., Steingrimsson, E., Diaz, R.J., Patapoutian, A., Merriam, J.R., and Lengyel, J.A. (1990). The *Drosophila* gene *tailless* is expressed at the embryonic termini and is a member of the steroid receptor superfamily. *Cell* *62*, 151–163.
- Price, J.V., Clifford, R.J., and Schupbach, T. (1989). The maternal ventralizing locus *torpedo* is allelic to *faint little ball*, an embryonic lethal, and encodes the *Drosophila* EGF receptor homolog. *Cell* *56*, 1085–1092.
- Rauen, K.A. (2013). The RASopathies. *Annu. Rev. Genomics Hum. Genet.* *14*, 355–369.
- Schejter, E.D., and Shilo, B.Z. (1989). The *Drosophila* EGF receptor homolog (*DER*) gene is allelic to *faint little ball*, a locus essential for embryonic development. *Cell* *56*, 1093–1104.
- Schweitzer, R., Shaharabany, M., Seger, R., and Shilo, B.Z. (1995). Secreted Spitz triggers the *DER* signaling pathway and is a limiting component in embryonic ventral ectoderm determination. *Genes Dev.* *9*, 1518–1529.
- Sutherland, D., Samakovlis, C., and Krasnow, M.A. (1996). Branchless encodes a *Drosophila* FGF homolog that controls tracheal cell migration and the pattern of branching. *Cell* *87*, 1091–1101.
- Toettcher, J.E., Weiner, O.D., and Lim, W.A. (2013). Using optogenetics to interrogate the dynamic control of signal transmission by the Ras/Erk module. *Cell* *155*, 1422–1434.
- Umehono, Y., Tasaki, J., Nishimura, Y., Hrouda, M., Kawaguchi, E., Yazawa, S., Nishimura, O., Hosoda, K., Inoue, T., and Agata, K. (2013). The molecular logic for planarian regeneration along the anterior-posterior axis. *Nature* *500*, 73–76.
- Urban, S., Brown, G., and Freeman, M. (2004). EGF receptor signalling protects smooth-cuticle cells from apoptosis during *Drosophila* ventral epidermis development. *Development* *131*, 1835–1845.

Developmental Cell, Volume 40

Supplemental Information

**The Spatiotemporal Limits
of Developmental Erk Signaling**

Heath E. Johnson, Yogesh Goyal, Nicole L. Pannucci, Trudi Schüpbach, Stanislav Y. Shvartsman, and Jared E. Toettcher

Supplementary Materials for

The spatiotemporal limits of developmental Erk signaling

H. Johnson*, Y. Goyal*, N. Pannucci, T. Schüpbach, S.Y. Shvartsman, J.E. Toettcher
Correspondence to: toettcher@princeton.edu

This PDF file includes:

Supplementary Methods
Figs. S1 to S4
Table S1
Captions for Movies S1 to S6

Supplementary Methods

Plasmids

The tRFP-SSPB-SOScat-P2A-iLID-CAAX expression cassette was first assembled using a PUWR backbone (Drosophila Genome Resource Center, #1281) as transfer vector. A DNA fragment corresponding to tRFP-SSPB was PCR amplified from pLL7.0: tgRFPt-SSPB WT (a gift from Brian Kuhlman, Addgene plasmid #60415) (Guntas, et al., 2015) using primers tRFP_F and SSPB_R (see table below). The SOScat fragment was PCR amplified from pHR-YFP-PIF-SOScat (Addgene plasmid #50851) using the primers SOScat_F and SOScat_R. The iLID-CAAX sequence was PCR amplified from pLL7.0: Venus-iLID-CAAX (a gift from Brian Kuhlman, Addgene plasmid #60411) (Guntas, et al., 2015) using primers iLID_F and iLID_R. The P2A sequence was introduced within the SOScat_R and iLID_F primers. The aforementioned three PCR fragments were then ligated into an EcoRI/XbaI-cut pUWR vector using In-Fusion assembly (Clontech). Sequence corresponding to the assembled tRFP-SSPB-SOScat-P2A-iLID-CAAX construct was subsequently PCR amplified in its entirety from the PUWR transfer vector using the primers pTiger_F and pTiger_R. The resulting PCR product was ligated into a KpnI/NheI-cut pTIGER vector (Ferguson, et al., 2012) using In-Fusion assembly. The final coding sequence of the pTIGER-tRFP-SOScat-P2A-iLID-CAAX construct was fully sequenced to ensure the absence of any mutations.

Primers used to construct OptoSOS plasmids

Primer Name	Primer Sequence (5'-3')
tRFP_F	cgggctgcaggaattatggtgtctaagggcgaagagctg
SSPB_R	agtggtgcatgaattcaccaccagcactaccaatattcagctcgcatag
SOScat_F	attcatgcaaccactgagattaccaagtctgaagtatatcg
SOScat_R	tccagcctgcttcagcaggctgaagttagtagctccgctccggtagagccatgtcggcctgtgt
iLID_F	ctgaagcaggctggagacgtggaggagaacctggacctgagttctggcaaccacactggaacg
iLID_R	ttgggtacgtctaggtgggagttgcccgcg
pTIGER_F	aggtcctgttcattggtaccgggctgcaggaattatggtgtctaagg
pTIGER_R	atgcatgcctgctagcattgggtacgtctaggtgggagttgcg

Fly procedures

Generation of transgenic flies and Stocks: Constructs described in 'plasmids' section were integrated into the 3rd chromosome using the ϕ C31-based integration system (Bischof, et al., 2007), at the Attp site estimated to be at 68A4. OregonR, Histone-GFP, Tor^{D4021/+} alleles were also used in the experiments. P(mata-GAL-VP16)mat67; P(mata-GAL-VP16)mat15 was used to drive iLIDnano expression in the early embryo (Hunter and Wieschaus, 2000). Flies were raised under standard conditions and crosses were

performed at 25°C unless otherwise specified.

Immunostaining and fluorescent in situ hybridization

Rabbit anti-dpErk (1:100; Cell Signaling), sheep anti-GFP (1:1000, Bio-Rad), sheep anti-digoxigenin (DIG) (1:125; Roche), and mouse anti-biotin (1:125; Jackson ImmunoResearch), rat anti-mCherry (1:1000; Life Technologies) and rat anti HA (1:100, Roche # 11-867-423-001) were used as primary antibodies. DAPI (1:10,000; Vector laboratories) was used to stain for nuclei, and Alexa Fluor conjugates (1:500; Invitrogen) were used as secondary antibodies.

Fluorescent imaging was done with a Nikon A1-RS scanning confocal microscope with a 20x objective. For pairwise comparisons of wild type and mutant backgrounds, embryos were collected, stained, and imaged together under the same experimental conditions. Error bars represent the standard error of the mean of embryo ages (x-axis) and normalized dpErk intensities (y-axis).

Cuticle preparation

Embryos were dechorionated after being aged for more than 30 hours. Dechorionated embryos were incubated overnight in a media containing lactic acid and Hoyer's medium (1:1) at 65C. Cuticle imaging was performed with Nikon Eclipse Ni at 10X objective.

Microscopy

For Figure 1 and S2C, bright-field and confocal microscopy was performed on a Nikon Eclipse Ti microscope with a Prior linear motorized stage, a Yokogawa CSU-X1 spinning disk, an Agilent laser line module containing 405, 488, 561 and 650 nm lasers, and an iXon DU897 EMCCD camera. For translocation experiments embryos were dechorionated in 50% bleach for 2 minutes and rinsed in water before mounting and imaging at 40x. Microscopy of fixed samples in figure 2 was performed using a Nikon A1 RS point-scanning confocal microscope (Princeton microscopy core). For cuticle staining, dark-field images were collected on a Nikon Eclipse Ni.

For the patterned illumination experiments in **Figure 3** and **Movie S3**, embryos were collected for 45 minutes, aligned on coverslip in a 3:1 mix of halocarbon 700/27 oil. The slide was then sandwiched with a Teflon window chamber using vacuum grease (a technique described in detail in (Kiehart, et al., 1994)). The Teflon chamber was positioned on a Prior Proscan III XY stage. Patterned optogenetic illumination was performed using a Mightex Polygon digital micromirror device using an X-Cite XLED 450 nm blue light source; regions of illumination were drawn as regions of interest (ROIs) in NIS Elements. 450 nm light was applied at 40% power for 100 msec to each embryo at 20x. All embryos were illuminated once every 40 sec starting 30 minutes after collection – at this imaging frequency, up to 30 embryos could be illuminated per experiment. Just before stimulation, DIC images of each embryo were collected with a

650 nm long-pass filter (Chroma) in the light path to prevent any light-induced SOScat activation. Embryos which were in late NC 14 or older were excluded from counts.

Temporal activation experiments

Embryos were collected for 45 minutes at 25 °C before being wrapped in foil and aged at room temperature for ‘X’ hours before stimulation (where ‘x’ is defined for specific experiments in the corresponding text and figure). They were then placed in blue LED containing foil wrapped boxes and stimulated for ‘Y’ hours before returning to the dark for 30+ hours (where ‘y’ is defined for specific experiments in the corresponding text and figure). To achieve lower activation levels the LEDs were toggled on for one second pulses at regular intervals using an Arduino microcontroller. Lethality was calculated by counting unhatched and empty eggshell cases on a random region of each plate.

Implementing OptoSOS using the Phy/PIF system in *Drosophila*

Our first effort to test OptoSOS function in flies took advantage of the Phy/PIF light-induced heterodimerization system we used in prior work in mammalian cells (Toettcher, et al., 2013; Toettcher, et al., 2011). We integrated two plasmids – pTIGER Phy-HA-CAAX and pTIGER mCherry-PIF-SOS – separately into two different fly lines, both under UAS control (fly injection performed by Best Gene Inc). Each was crossed with the GAL4 driver fly line (P[mata-GAL-VP16]mat67; P[mata-GAL-VP16] mat15) to observe expression of the components individually. Expression of each component was observed by HA and mCherry antibody staining (**Figure S1A**).

For introducing PCB to embryos via microinjection, embryos were dechorionated using 50% bleach before being aligned along the edge of a coverslip. The embryos are then desiccated for 12 minutes before a 3:1 mix of 700/27 halocarbon oil is added to prevent further evaporation. The embryos were then injected for about 5% of the embryos volume with PCB dissolved in PBS at a 1:10 dilution. As PCB is autofluorescent at infrared wavelengths, we excited it using 647 nm laser to confirm that it was successfully injected into the embryos (**Figure S1B**). It should be noted that this is a convenient way to test for proper Phy localization, because PCB-bound Phy is fluorescent in the Cy5 channel and can be seen localized to membranes in Phy-CAAX expressing embryos.

Screening for light-induced Erk activation in *Drosophila* S2 cells

We cultured S2 cells (a gift from Elizabeth Gavis, Princeton University) in Schneider’s *Drosophila* media (SDM) supplemented with 10% FBS on polylysine coated flasks. S2 cells were then plated in polylysine coated plates and allowed to adhere. We then transfected each construct (pTIG-UAS-MEK E203K + pTIG-UAS-GFP+ pMT-GAL4 (Klug, et al., 2002); pTIG-UBProm- tRFP-SSPB + pTIG-UBProm-iLID-CAAX; or pTIG-UBProm- tRFP-SSPB-SOS-P2A-iLID-CAAX) using Lipofectamine 2000 following the manufactures protocol and keeping the total DNA constant. The MEK construct is co-transfected with GFP to infer which cells are expressing it.

Three hours after transfection the media was replaced with serum free SDM containing 1 mM CuSO₄ to induce they GAL4 construct and incubated at room temperature overnight. The next day, wells were either left unstimulated or stimulated with blue light or inhibitor for 30 minutes before fixing by adding an amount equal media volume in the well of 1% paraformaldehyde for 5 minutes. The media/ paraformaldehyde is then removed and replaced with ice cold methanol and incubated for 10 mins at -20 °C, The wells are then blocked using IF buffer (PBS+10%FBS) for 1 hour at room temperature. After the blocking, cells are incubated at 4 °C overnight in 1:200 dpErk antibody in IF-T butter (IF butter with 3µL/mL Triton-X). The next day, cells are washed 3 times with IF-T before adding 1:400 secondary AB in IF-T. After incubation for 1 hour at room temperature, cells are washed three times again with IF-T before imaging. Relative dpErk levels were quantified in MATLAB by calculated the mean dpErk intensity in the transfected cells (segmented by GFP or tRFP) in each well and comparing with that of untransfected cells. We observed a significant increase in dpErk in light stimulated OptoSOS S2 cells comparable with those which contain the constitutively active E203K MEK (**Figure S1C**).

SOScat translocation can be controlled by the duration or intensity of illumination

Two mechanisms can in principle be used to control the extent of translocation of a protein heterodimerization system – the intensity of light applied, and the duration of a pulse of light. We found that both are equally capable of limiting the extent of SOScat translocation (**Figure 1B**; **Figure S1D**). Importantly, varying the duration of maximum-intensity light pulses is a highly precise way to vary intensity that does not depend sensitivity on the distance between light source and embryo (as long as the intensity is above a threshold). We therefore used pulse-width modulation to drive intermediate levels of activation in subsequent experiments.

SOScat expression and translocation persist throughout embryogenesis

Our constructs are expressed from maternally-driven Gal4, so transcription of new iLID-CAAX and SSPB-SOScat mRNA ends when the egg is laid. This is excellent for expression in the early embryo (as mRNA and protein will be present prior to the initiation of zygotic transcription) but potentially poses a problem for expression of the OptoSOS system in late embryogenesis. To test for the duration of light sensitivity during embryogenesis, we imaged SOScat translocation and Erk phosphorylation in late embryos. Even at 12 hours post fertilization, we observed SOScat expression and light-induced membrane translocation (**Figure S1E**) as well as light-induced Erk phosphorylation (**Figure 2D**). To further characterize our ability to activate Erk over time, we quantified the total dpErk intensity in illuminated OptoSOS embryos at various points in development and normalized to the dpErk levels of similarly staged wild-type embryos (**Figure S2F**). We observed that at all stages tested, we were able to broadly activate dpErk phosphorylation to levels ~3x higher than those seen in wild-type embryos (note that wild-type embryos at each time point tested exhibit localized regions of high endogenous Erk activity).

To quantitatively test how dpErk levels compare between 12 h old OptoSOS and WT embryos, we computationally measured the dpErk intensity along a line scan through the brightest denticle patterning in both wt and OptoSOS illuminated embryos (**Figs 2D & 2E**). While the endogenous pattern is still visible on top of light-induced Erk in OptoSOS embryos at this stage, the minimum dpErk intensity in OptoSOS embryos is still two-fold higher than that of the maximum dpErk level in wild-type embryos, indicating that any decrease in expression of our optogenetic system does not significantly decrease our ability to activate Erk.

To ensure that light was capable of fully penetrating embryos to active Erk in internal tissues, we imaged internal dpErk levels in 12 h old embryos in mid-embryo confocal slices (**Fig S2E**). These mid-plane slices of embryos show internal activation which is as high or higher than on the surface, indicating that we are not limited in penetration depth with the light intensities used throughout our study.

Image processing for quantifying recruitment in early embryos

Since translocation of the tRFP-SSPB-SOScat causes a visible change in localization and intensity we sought to develop a robust method to quantify the relative amount of translocation in response to light. As the embryo develops, cells divide and rearrange, the focal plane changes, and the fluorescence intensity can vary. Furthermore, tRFP-SSPB-SOScat is excluded from nuclei except during cell division causing non-uniformities. To work around these challenges we took advantage of the ability to locally stimulate each embryo so that we can normalize by a non-stimulated area in the same plane at the same state. A metric which encompasses the relative translocation is the membrane to cytosolic ratio of tRFP-SSPB-SOScat. This is approximated by the ratio of the intensity gradient of tRFP-SSPB-SOScat in the light and dark states. To calculate this we first apply a 4 by 4 pixel Gaussian filter to the intensity image (I) to prevent contributions to the gradient from pixel-to-pixel noise (*i.e.* gradients that are not caused by transitions from membrane to cytosol). Next, we approximated the gradient of the image using a Sobel gradient operator. We then integrated this gradient over the area of the image and normalized by the size of the region.

$$\textit{Translocation} \approx \frac{1}{A} \iint \nabla I$$

This same operation is then performed in a dark region in the same image and the result is normalized by the value, to give the final result for that frame (**Figure S1F**).

Light-induced Erk activation in pole cells

During normal embryogenesis Erk signaling is absent in pole cells during NC 9 -14 (Deshpande, et al., 2004). However, after broad illumination of OptoSOS embryos with light we observed even higher activation of Erk activity in the germ cells than the in somatic tissue. (**Figure S2C**). Given that the Erk signal is normal very low in pole cells at this stage and that Erk activity in pole cells plays a role in overriding transcriptional repression (Deshpande, et al., 2004), we hypothesized that high levels of Erk might have

an adverse effect on germline development. Embryos where Erk was activated in the tail for 2 hours during terminal patterning were allowed to develop to adults. These flies were then mated to determine fertility, and ovary dissections were performed after adding yeast to the fly diet for 3 days. Strikingly, in the 17 flies tested all were capable of producing offspring, and the ovaries were full and indistinguishable from wildtype. Our results thus demonstrate that even the high levels of Erk activity induced by light (**Figure S2C**) are insufficient to remove pole cells' transcriptional repression.

Titration of Erk activity, segmentation defects, and lethality using pulsed inputs

To characterize the overall lethality of light-induced Erk at different times during embryogenesis (**Figure S4**), we applied increasing durations of light stimulation to the early embryo and quantified the number of hatched or unhatched eggshells. We observed an abrupt increase in lethality after ~2 h of continuous light stimulation, and virtually all OptoSOS embryos were nonviable after 4 h of continuous light stimulation (**Figure S4A**). Exposing embryos to 2 h of light at different times during embryogenesis revealed that lethality decreased as the stimulus was applied at later times, with ~25% of embryos surviving a 2 hour continuous blue light stimulus delivered from 4-6 hours after fertilization (**Figure S4B**).

We next sought a method to titrate light intensity to test if a single light dose could give rise to differential sensitivity to Erk in early vs late embryos. Because it is difficult to deliver perfectly uniform light intensity over large exposure areas, we found that titrating the duration of a pulsed bright light input (a technique known as pulse width modulation) was preferable to titrating its intensity. We expected dimerization and downstream Ras/Erk signaling will “average out” pulses on a 1-2 min timescale, resulting in an intermediate, steady-state level of activation (Toettcher, et al., 2013). We therefore pulsed at different rates (once per 30 sec, once per 60 sec or once per 120 sec).

Figure S4E shows that different frequencies of light pulses delivered after the first 4 hours of embryogenesis indeed induced different levels of lethality. We verified that our blue light input was *itself* not toxic, as even 5 h of continuous light did not induce any lethality or developmental phenotypes in wild-type embryos (**Figure S4A**). We observed a difference in light-induced lethality in early- vs late-stimulated embryos across all stimulus frequencies tested, and a pronounced difference in body segment defects even when overall lethality was high (**Figure S4B**; **Figure 4D**).

Effect of ectopic Erk activation on tracheal branching

During stage 11 branchless patterns Erk in cells near the tracheal sac by activating the breathless receptor, an FGFR homolog. These cells then migrate to form tracheal branches in the following stages. Ectopic activation of breathless at this stage has been shown to disrupt this migration and the subsequent branch formation (Gabay, et al., 1997; Sutherland, et al., 1996). Given that Erk may play a role in this process, we sought to see if branch formation would be disrupted in the surviving larva from the 4-24hr activation in **Figure 4E**. Prior to imaging, larvae were added to a 50% glycerol water

solution and heated to 56 °C for ~30s to prevent movement during imaging.

To image tracheae we used a combination of DIC and autofluorescence imaging. We found that the tracheae were quite autofluorescent in response to 450nm light, likely due to tracheal chitin. Images were thus created by taking confocal z-stacks of larvae using a 40X oil immersion objective, and then performing a minimum intensity projection on the DIC images and a maximum intensity projection on the 450 autofluorescence images to obtain the images shown in **Figure S4E**. More than 20 larvae were imaged in both the case of WT and OptoSOS larvae; in all cases, no gross branching defects were observed, in contrast to what is obtained in response to ectopic branchless expression (Sutherland, et al., 1996). Our results suggests that branching morphogenesis may require combinatorial control of multiple Breathless/Branchless dependent pathways, an interpretation supported by recent work showing that mutants which affect phospholipid production can also give increased terminal branched phenotypes (Ghabrial, et al., 2011). Future studies will be needed to determine the relative roles of each signal downstream of breathless in tracheal branching.

In situ hybridization to monitor light-induced alteration in target gene expression

In order to understand how ectopic Erk could give such strong early phenotypes but not late we used fluorescence *in situ* hybridization to look at gene expression domains at various points in embryogenesis in response to OptoSOS activation (**Figure 4**). Embryos were collected to age in the dark for the appropriate time before stimulating (*hkb*, *ill*, *aos*, and *otd* 1 hr of light stimulation; *ind* 0.75 hr of light stimulation) fixed in the presence of blue light. FISH was performed as described previously (Lim, et al., 2013). We observed a grading of expansion, decreasing as embryo age increased, consistent with a hypothesis of increased regulation later in development.

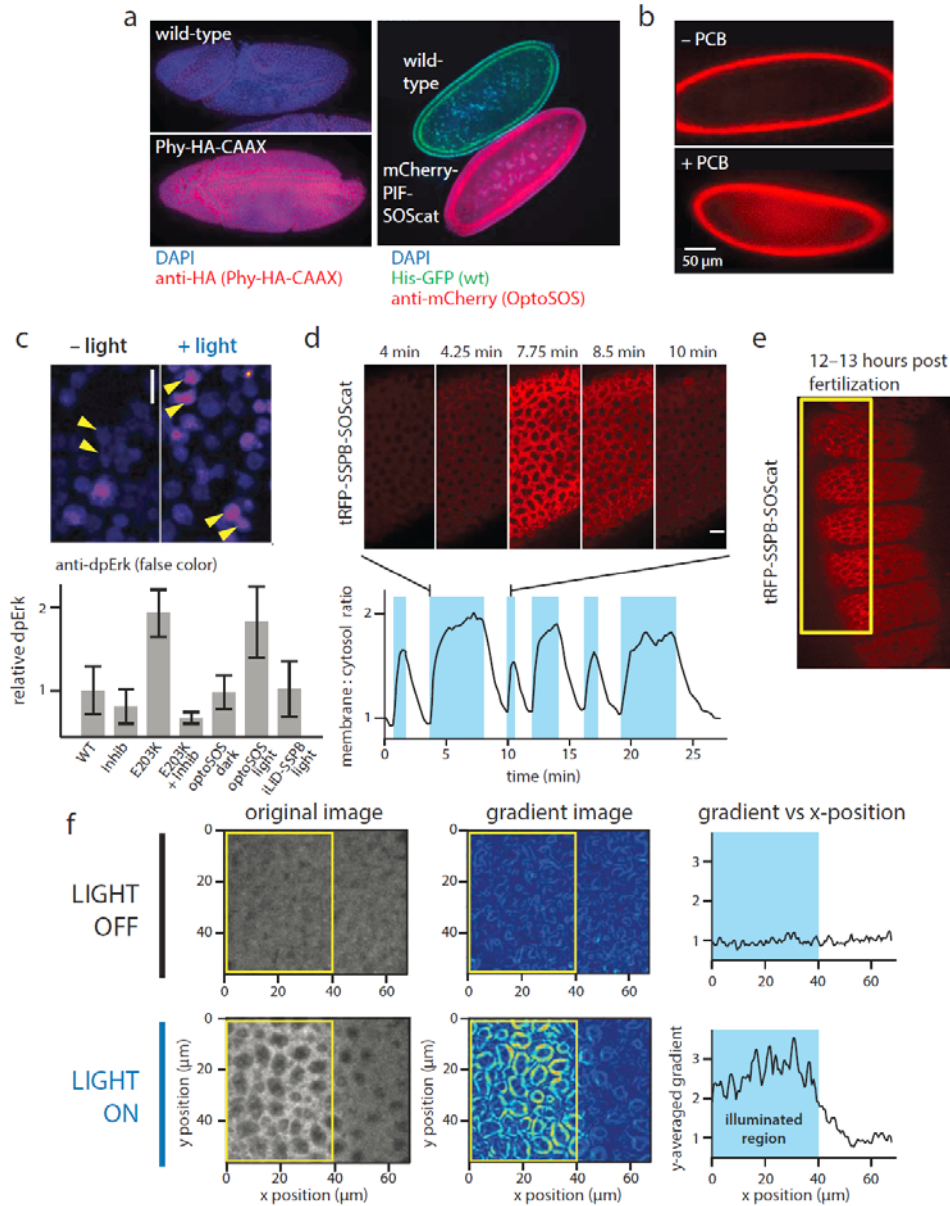


Figure S1, related to Figure 1. Developing and characterizing the OptoSOS system in *Drosophila*. (A) Staining of Phy-HA-CAAX and mCherry-PIF-SOScat embryos for expression of the components. (B) 650 nm fluorescence with/without PCB injection. (C) dpErk staining in S2 cells with and without light. OptoSOS-expressing cells are marked with yellow arrows (top). Conditions include: WT, overexpression of GOF MEK E203K, MEK inhibitors PD0325901 and U0126, with/without light stimulation as well as an optogenetic construct omitting the SOScat domain. Error bars: SD of n = 4, 4, 4, 4, 5, and 6 wells for the conditions listed. (D) Montage and quantification of translocation for varying stimulation dynamics, light is pulsed for 100ms every 15 seconds in shaded regions. (E) Translocation during late embryogenesis; light was presented only in the yellow box. (F) Example of the method used to quantify translocation. Stimulation occurs within the boxed region.

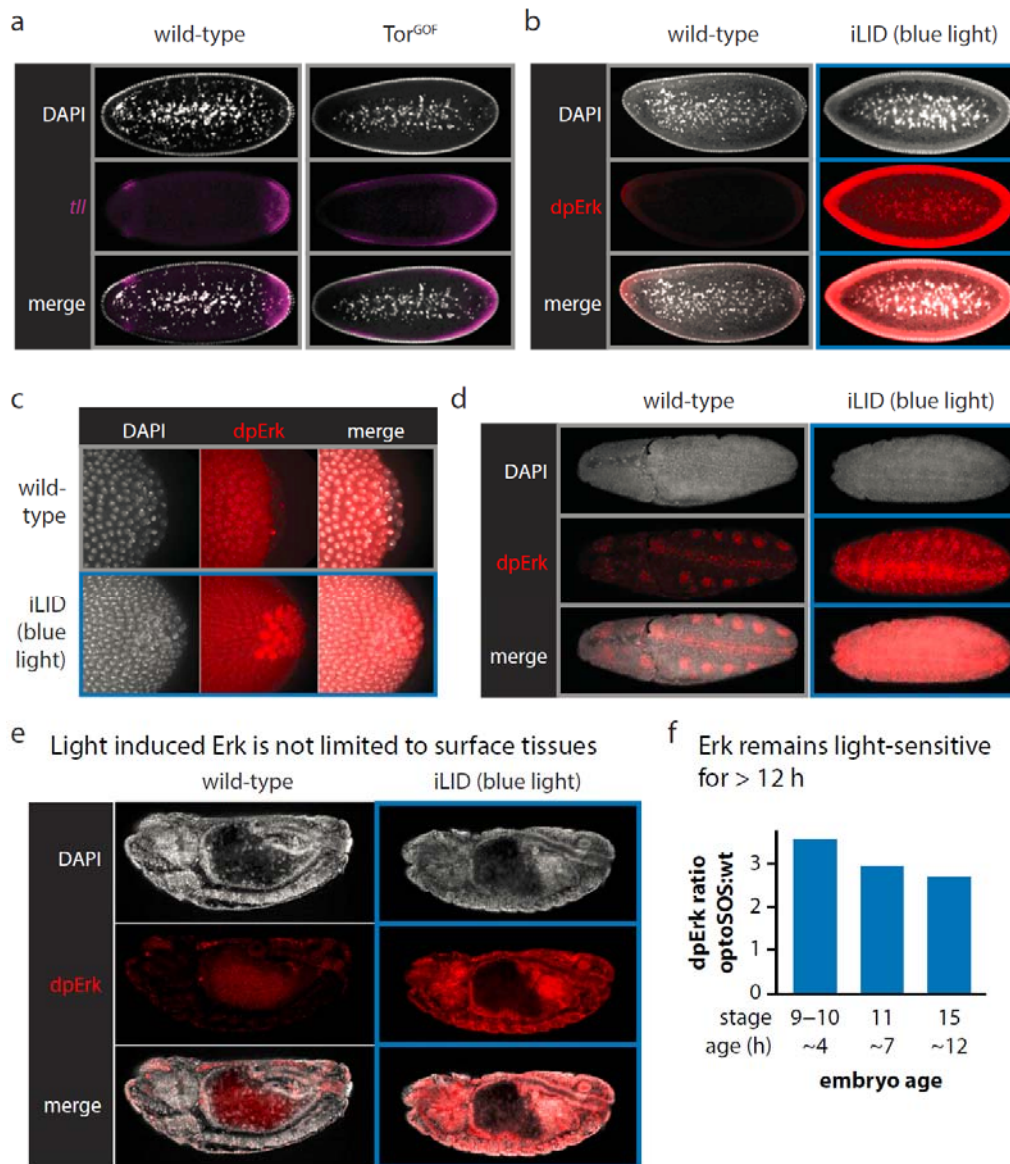


Figure S2, related to Figure 2. Light-induced Erk pathway responses in OptoSOS flies. (A) Midsection images showing expansion of tailless staining at NC 14 embryos expressing mutant Torso D4021 compared to wild type. (B) Midsection images of Erk staining used for quantification shown in **Figure 2B**. (C) Close-up images of pole cells from wild type and OptoSOS embryos in **Figure 2B**. (D) dpErk staining of 5-6 hour old wild type and OptoSOS embryos. (E) dp-Erk midsections for the 12 h old wild-type and OptoSOS embryos shown in **Figure 2D**. (F) Ratio of total dp-Erk staining in WT and light-illuminated OptoSOS embryos over time during development.

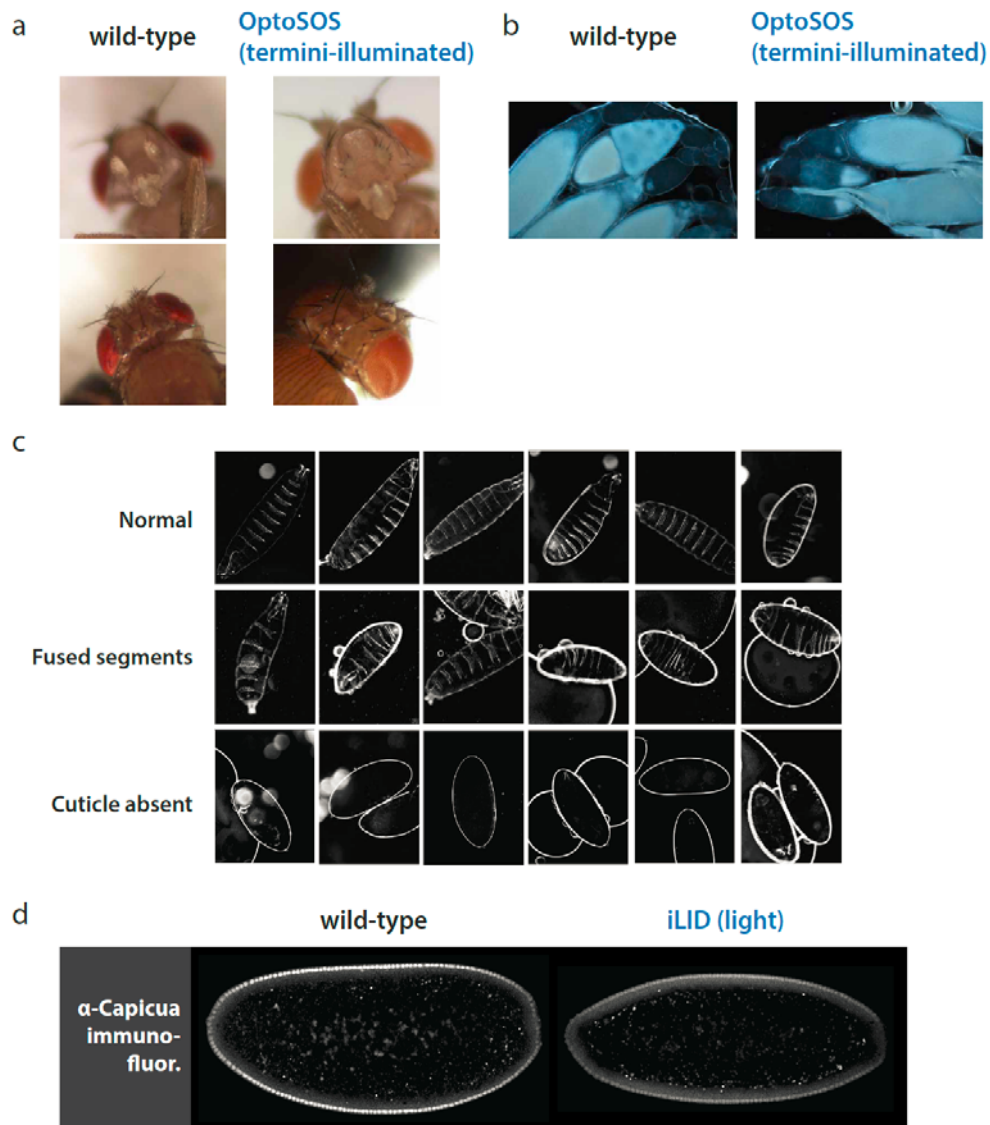


Figure S3, related to Figure 3. Characterizing phenotypes in illuminated OptoSOS flies. (A,B) Phenotypic consequences of illumination at the termini during early embryogenesis. OptoSOS or wild-type flies were illuminated at the termini as in Figure 3 and allowed to develop to adulthood. Head structures (A) and ovary development (B) from each group were characterized. (C) Examples of the three cuticle phenotype classifications from various conditions after light stimulation. Those embryos with 8 separate cuticles are considered “normal”, many but not all of these are hatched. Embryos are classified as “fused” if it contains 1-7 segments or if the segments are connected. “Cuticle absent” is for embryos which have no visible cuticles; they may however have tail or head structures. (D) Full embryo image of the Cic staining shown in **Figure 3G**.

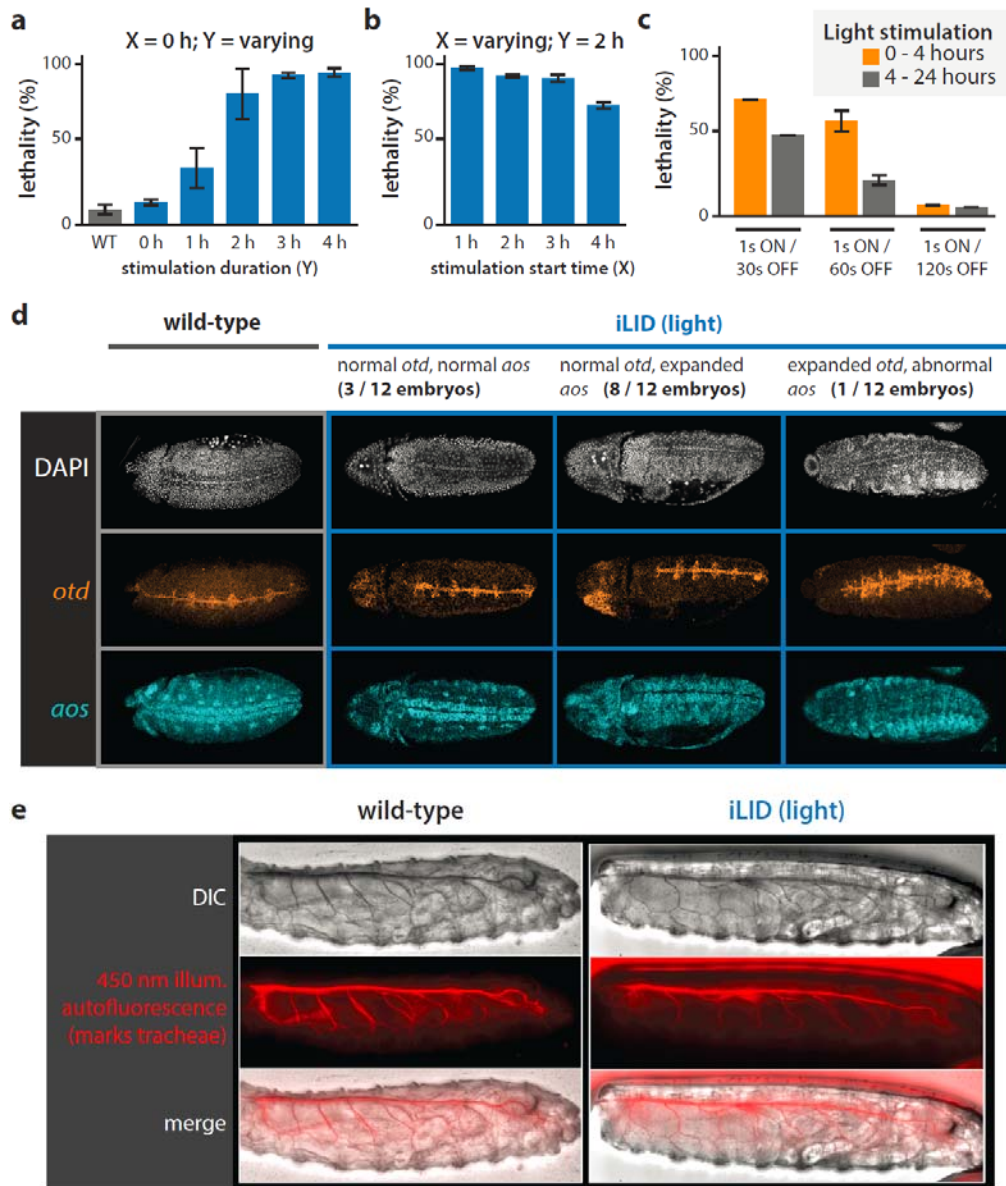


Figure S4, related to Figure 4. Identifying the temporal window of sensitivity to ectopic Erk activation. (A) Lethality for varying stimulation lengths used in Figure 4C (mean + SD). (B) Lethality for varying age time with 2 hour stimulation using high-intensity light, as used in Figure 4D (mean + SD). (C) Effect of titration of activation levels on lethality. Levels are reduced by increasing the window between 1 second pulses. The middle level (1s on 60s off) is the same as shown in Fig 4e. Error bars show mean + SD. (D) Different *otd* and *aos* expression patterns observed by FISH as in **Figure 4F**. (E) Minimum (DIC) or maximum (autofluorescence) intensity projections of tracheae in surviving larva from the experiment in **Figure 4E**.

Table S1, related to Figures 2-4.

Number of embryos and replicates used in each experiment.

Figure	# of embryos	# of replicates
2b	WT: n=6; OptoSOS light: n=9; OptoSOS dark: n=13	2
3b	n > 40 embryos per condition	3+ per condition
3c	n > 40 embryos per condition	3+ per condition
3e	dark: n=24; anterior: n=33; middle: n=18; posterior: n=37	3+ per condition
3g	WT: n=21; iLID: n=14	1
4c	n = 88, 87, 121, 36, 191, 70 across conditions listed	1
4d	n = 146, 88, 43, 118 across conditions listed	1
4e	n = 524, 271 total embryos analyzed	3+ per condition
S4a	n = 520, 241, 283, 94, 354, 210 across conditions listed	2-5 replicates per condition
S4b	n = 200+ per condition	2-4 replicates per condition
S4c	n = 124, 104, 524, 271, 42 and 68 across conditions listed	1-5 replicates per condition

Movie S1, related to Figure 1

Titration of membrane recruitment of tRFP-SSPB-SOScat with varying light intensities. Time (in hours:minutes format) is shown as an overlay on the figure. tRFP images are shown as a sequence of different light intensities was applied to a single embryo. Quantification of the translocation from this movie is shown in Figure 1B.

Movie S2, related to Figure 1

Achieving precise spatial control of membrane SOScat on a ~1 min timescale. A digital micromirror device was used to draw an arbitrary pattern (here a series of text letters) on a live embryo, while tRFP images were simultaneously obtained. Time (in hours:minutes:seconds format) is shown as an overlay on the figure. A translocation pattern emerges within 1 min and decays within 2 min after removal of light stimulus. Still images from this movie shown in Figure 1C.

Movie S3-S4, related to Figure 3

Timecourse of development for OptoSOS embryos stimulated in their center regions with light. Embryos were stimulated in the middle with 80 μm wide light stimuli for 2 hours prior to the start of imaging (shaded blue regions indicate the areas where light was delivered). Just before imaging was initiated, the blue light was turned off. Embryos were imaged over time (~8 hours) and exhibit local tissue contraction at the site of illumination during the first 2 hours of imaging, as well as pronounced defects in gastrulation and subsequent development.

Movie S5, related to Figure 3

Timecourse of development of an OptoSOS embryo in response to uniform light exposure. The embryo was stimulated with uniform blue light continuously through the movie. Nuclear cycles 9-14 proceed normally, but during gastrulation the posterior side of the embryo (the right-hand side of movie) contracts and pushes the yolk entirely to the anterior (left-hand) side.

Movie S6, related to Figure 3

Timecourse of development of a wild-type embryo in response to uniform light exposure. Movie was acquired in the same manner as Movie S5. Development proceeds normally through nuclear cycles 9-14 and gastrulation.

References

- Bischof, J., Maeda, R.K., Hediger, M., Karch, F., and Basler, K. (2007). An optimized transgenesis system for *Drosophila* using germ-line-specific phiC31 integrases. *Proceedings of the National Academy of Sciences of the United States of America* 104, 3312-7.
- Casci, T., Vinos, J., and Freeman, M. (1999). Sprouty, an intracellular inhibitor of Ras signaling. *Cell* 96, 655-65.
- Deshpande, G., Calhoun, G., and Schedl, P. (2004). Overlapping mechanisms function to establish transcriptional quiescence in the embryonic *Drosophila* germline. *Development* 131, 1247-57.
- Ferguson, S.B., Blundon, M.A., Klovstad, M.S., and Schupbach, T. (2012). Modulation of gurken translation by insulin and TOR signaling in *Drosophila*. *J Cell Sci* 125, 1407-19.
- Gabay, L., Seger, R., and Shilo, B.Z. (1997). MAP kinase in situ activation atlas during *Drosophila* embryogenesis. *Development* 124, 3535-41.
- Ghabrial, A.S., Levi, B.P., and Krasnow, M.A. (2011). A systematic screen for tube morphogenesis and branching genes in the *Drosophila* tracheal system. *PLoS genetics* 7, e1002087.
- Guntas, G., Hallett, R.A., Zimmerman, S.P., Williams, T., Yumerefendi, H., Bear, J.E., and Kuhlman, B. (2015). Engineering an improved light-induced dimer (iLID) for controlling the localization and activity of signaling proteins. *Proceedings of the National Academy of Sciences of the United States of America* 112, 112-7.
- Hunter, C., and Wieschaus, E. (2000). Regulated expression of nullo is required for the formation of distinct apical and basal adherens junctions in the *Drosophila* blastoderm. *The Journal of cell biology* 150, 391-401.
- Kiehart, D.P., Montague, R.A., Rickoll, W.L., Foard, D., and Thomas, G.H. (1994). High-resolution microscopic methods for the analysis of cellular movements in *Drosophila* embryos. *Methods Cell Biol* 44, 507-32.
- Klug, K.M., Alvarado, D., Muskavitch, M.A., and Duffy, J.B. (2002). Creation of a GAL4/UAS-coupled inducible gene expression system for use in *Drosophila* cultured cell lines. *Genesis* 34, 119-22.
- Lim, B., Samper, N., Lu, H., Rushlow, C., Jimenez, G., and Shvartsman, S.Y. (2013). Kinetics of gene derepression by ERK signaling. *Proceedings of the National Academy of Sciences of the United States of America* 110, 10330-5.
- Nakamura, A., and Seydoux, G. (2008). Less is more: specification of the germline by transcriptional repression. *Development* 135, 3817-27.
- Sutherland, D., Samakovlis, C., and Krasnow, M.A. (1996). branchless encodes a *Drosophila* FGF homolog that controls tracheal cell migration and the pattern of branching. *Cell* 87, 1091-101.
- Toettcher, J.E., Gong, D., Lim, W.A., and Weiner, O.D. (2011). Light-based feedback for controlling intracellular signaling dynamics. *Nature methods* 8, 837-9.
- Toettcher, J.E., Weiner, O.D., and Lim, W.A. (2013). Using optogenetics to interrogate the dynamic control of signal transmission by the Ras/Erk module. *Cell* 155, 1422-34.